Relativistic mean field plus exact pairing approach to open shell nuclei

Wei-Chia Chen,* J. Piekarewicz,† and A. Volya‡
Department of Physics, Florida State University, Tallahassee, Florida 32306, USA
(Received 19 November 2013; published 27 January 2014)

Background: Pairing correlations play a critical role in determining numerous properties of open shell nuclei. Traditionally, they are included in a mean field description of atomic nuclei through the approximate Bardeen-Cooper-Schrieffer or Hartree-Fock-Bogoliubov formalism.
Purpose: We propose a new hybrid "relativistic mean field plus pairing" approach in which pairing is treated exactly so the number of particles is conserved. To verify the reliability of the formalism, we apply it to the study of both ground-state properties and isoscalar monopole excitations of the tin isotopes.
Methods: Accurately calibrated relativistic mean field models supplemented by an exact treatment of pairing correlations are used to compute ground-state observables along the isotopic chain in tin. In turn, ground-state densities are used as input to the calculation of giant monopole resonances through a constrained-relativistic approach.
Results: We compute a variety of ground-state observables sensitive to pairing correlations as well as the evolution of giant monopole energies along the isotopic chain in tin. Whereas ground-state properties are consistent with experiment, we find that pairing correlations have a minor effect on the giant monopole energies.
Conclusions: A new mean field plus pairing approach is introduced to compute properties of open shell nuclei. The formalism provides an efficient and powerful alternative to the computation of both ground-state properties and monopole energies of open shell nuclei. We find ground-state properties to be well reproduced in this approach. However, as many have concluded before us, we find that pairing correlations are unlikely to provide an answer to the question, "Why is tin so soft?"

DOI: 10.1103/PhysRevC.89.014321 PACS number(s): 21.10.Dr, 21.10.Gv, 21.10.Re, 21.60.Jz

I. INTRODUCTION

Since the early days of nuclear physics, there has been ample experimental evidence in support of nuclear pairing in atomic nuclei [1,2]. Indeed, already in 1950 Maria Goeppert Mayer suggested that an even (odd) number of identical nucleons occupying the same single-particle orbit of angular momentum j will couple to a total angular momentum of $J = 0$ ($J = j$) [1]. One remarkable consequence of such an assumption is that all even-even nuclei are predicted (and so far observed) to have a ground state with a total angular momentum of $J = 0$ and a ground-state energy that is significantly lower relative to that of its odd-nucleon neighbors.

Pairing correlations involve the binding of identical nucleons moving in time-reversed orbits around the Fermi surface. In general, the imprint of pairing correlations is observed in a variety of nuclear properties, such as binding energies, one-nucleon separation energies, single-particle occupancies, excitation spectra, level densities, moments of inertia, and low-lying collective modes, among others [3]. In recent years, the focus of nuclear structure has shifted from the valley of stability to the boundaries of the nuclear landscape. Indeed, it is now possible to both synthesize and probe the structure of *exotic nuclei*, particularly neutron-rich and neutron-deficient nuclei [4,5]. Moreover, the ongoing quest for *superheavy elements* continues. This quest involves a sustained effort on both their synthesis and theoretical predictions of novel shell structures and new magic numbers [6,7]. It is widely recognized that pairing correlations play a critical role along these new frontiers.

Theoretical treatments on nuclear pairing can be classified into two groups: one approximate and the other exact. The approximate approaches followed the seminal work of Bardeen, Cooper, and Schrieffer (BCS) [8] on superconductivity in condensed-matter physics that were extended shortly after to the nuclear domain by Bohr *et al.* [9], Belyaev [10], and Migdal [11]. Since then, methods combining a Hartree-Fock formalism with BCS theory (HF + BCS) have been developed and widely implemented [12,13]. Although quite successful for macroscopic systems, BCS theory suffers from two main disadvantages when applied to finite nuclei. First, the BCS formalism does not conserve number of particles. This is not a serious issue for macroscopic systems containing 10^{23} particles, but it certainly becomes relevant for small systems like atomic nuclei. Second, for nuclei whose single-particle-energy spacing around the Fermi surface is greater than the typical pairing strength, the BCS formalism generates trivial solutions. These drawbacks complicate the identification of weakly bound nuclei near the drip line, as the whole concept of drip line becomes unclear when the exact number of particles is unknown. A more sophisticated approach that incorporates pairing correlations in a mean field framework is the Hartree-Fock-Bogoliubov (HFB) formalism [14]. In the HFB approach the (short-range) particle-particle channel associated with pairing correlations is treated on equal footing as the (long-range) particle-hole channel associated with the

*wc09c@my.fsu.edu
†jpiekarewicz@fsu.edu
‡volya@physics.fsu.edu

conventional HF description [15]. This technique has been successfully applied to stable and weakly bound nuclei in both the nonrelativistic [4,16,17] and relativistic domains [18–21]. However, the violation of particle number remains an important drawback of the HFB formalism. To overcome such difficulty, a complicated prescription, either approximate or exact, is often invoked to project out the state containing the desired number of particles [22–24]. Unfortunately, such a prescription along with many other ideas have been met with limited success. Meanwhile, a variety of new approaches aimed to solve the pairing problem *exactly* were proposed, primarily by Richardson [25–27]; see also Ref. [28] and references contained therein. For example, in the Richardson method the large-scale diagonalization of a many-body Hamiltonian in a truncated Hilbert space is reduced to a set of coupled algebraic equations with a dimension equal to the number of valence particles. Moreover, exact solutions to a generalized pairing problem using sophisticated mathematical tools, such as an infinite-dimensional algebra [29], have also been obtained. However, due to their intrinsic complexity these formal methods, although exact, are difficult to implement in realistic situations. Perhaps the most promising method to solve the pairing problem exactly is the one based on *quasispin symmetry*, first discovered by Racah in the 1940s [30,31]. By exploiting the underlying quasispin symmetry, it is possible to express the general pairing Hamiltonian in terms of quasispin operators that are far easier to cope with and manipulate [32,33]. The formalism was pushed one step further in Ref. [34] by transforming from the quasispin scheme into the seniority scheme, where the physical picture becomes clearer and the simplicity and practicality of the method were explicitly demonstrated. Further, it was suggested that a selfconsistent approach based on the combination of a mean field plus exact pairing formalism represents a promising alternative to large-scale diagonalization [35]. It is precisely the goal of the present contribution to implement and examine the power of this promising alternative.

In this work we introduce a new hybrid approach to study the properties of open shell nuclei. The approach is based on the combination of an accurately calibrated relativistic mean field (RMF) model and an exact treatment of pairing correlations. In the RMF theory the underlying nucleon-nucleon (NN) interaction is mediated by various "mesons" of different spin, parity, and isospin [36–38]. With ever increasing sophistication, the RMF theory has been extremely successful in describing ground-state properties of even-even nuclei all throughout the nuclear chart [39,40]. Pairing correlations have been incorporated into the RMF approach by adopting either a BCS or HFB formalism; see Refs. [18,19] and references contained therein. However, these approaches inevitably suffer from the aforementioned difficulties related to the violation of particle number. To circumvent this problem we propose the exact pairing (EP) approach of Ref. [34] to address the physics of open shell nuclei. The combination of RMF plus EP (RMF + EP) is both natural and straightforward to implement. Indeed, single-particle energies generated from the RMF approximation are the only input required by the EP algorithm to predict the occupancies of the valence orbitals. In turn, these new (fractional) occupancies modify the resulting single-particle spectrum—which is then fed back into the EP algorithm. This process continues until self-consistency is achieved. This combination of shell-model-like configuration interaction and relativistic mean field techniques is similar to many previously used methods, such as a combination of a Woods-Saxon potential and pairing [41], the shell-model-like approach (SLAP) developed in Ref. [42] with a particle-number-conserving technique for pairing correlations [43], and an exact diagonalization of the pairing part of interaction combined with a Skyrme density functional as in Ref. [35]. A large body of work with similar techniques applied in various physical situations can also be found in Ref. [44] and references contained therein. However, given that the main focus of this contribution is to examine the impact of pairing correlations on the structure and dynamics of semi-magic spherical nuclei, additional effects associated with deformation, Coriolis terms, and time-reversal symmetry in the noninertial rotating frame will be avoided altogether. Moreover, as we demonstrate later, the quasispin symmetry discussed in Sec. II B provides a substantial numerical advantage in this spherically symmetric limit.

We illustrate the power and utility of this combined RMF + EP approach by computing ground-state properties and giant-monopole energies for the tin isotopes. With an assumed closed shell structure for both ^{100}Sn and ^{132}Sn, the tin isotopes serve as a good arena for examining pairing correlations. In particular, we examine a few ground-state observables that highlight the critical role of pairing correlations, such as the odd-even staggering in the neutron separation energy. However, we are particularly interested in examining the impact (if any) of pairing correlations on the softening of the isoscalar giant monopole resonance (GMR). The GMR, also known as the nuclear *breathing mode*, is a radial density oscillation that provides a unique access to the experimentally inaccessible incompressibility of neutron-rich matter—a fundamental property of the equation of state. The distribution of isoscalar monopole strength has been traditionally measured using inelastic α scattering at very small angles [45]. Indeed, the distribution of monopole strength has been measured in ^{90}Zr, ^{116}Sn, ^{144}Sm, and ^{208}Pb [46–49] and, with the possible exception of ^{116}Sn, is accurately reproduced by mean field plus random-phase-approximation (RPA) calculations. However, more recent experimental studies of GMR energies along the isotopic chains in both tin [50,51] and cadmium [52] have revealed that the softening observed in ^{116}Sn is endemic to both isotopic chains [53,54]. A popular explanation behind this anomaly is the critical role that pairing correlations play in the physics of these superfluid nuclei [55–59]. Although the conclusions have been mixed and seem to depend on the character of the pairing force, it appears that pairing correlations are unlikely to provide a definite answer to the question, "Why is tin so soft?" Here too we address this critical question within the context of the RMF + EP approach. In particular, we apply the RMF + EP approximation to calculate the relevant ground-state properties required to compute the centroid energies of the tin isotopes from the recently implemented constrained-RMF approach [60]. We conclude, as many have done before us, that pairing correlations have a minor effect on the GMR energies of the tin isotopes.

The manuscript has been organized as follows. In Sec. II we outline separately the RMF and EP approaches. Although the description and implementation of both of these techniques have been discussed in detail elsewhere [see Refs. 34,61, and references contained therein], a brief review is provided in an effort to keep the manuscript self-contained. In particular, Sec. II puts special emphasis on the implementation of the EP approach on top of an RMF approximation. In Sec. III we display results obtained with the newly developed RMF + EP approach for some selective sets of ground-state observables and GMR energies along the isotopic chain in tin. Finally, we offer our conclusions in Sec. IV.

II. FORMALISM

In this section we briefly outline the formalism required to compute ground-state properties and GMR energies in an RMF + EP approach. We start by reviewing the general features of the RMF theory and then proceed to a discussion of the exact pairing approach and how to merge them together. We finish this section by describing how the RMF + EP framework may serve as input to the constrained-RMF approach to compute GMR energies.

A. Relativistic mean field theory

In the RMF theory a nucleus is described in terms of protons and neutrons interacting through the exchange of "mesons" of various spins, parities, and isospins. The interactions among the particles can be described by an effective Lagrangian density given as follows [36–38,62,63]:

$$\begin{aligned}\mathscr{L}_{\rm int} = \bar{\psi}\left[g_{\rm s}\phi - \left(g_{\rm v}V_\mu + \frac{g_\rho}{2}\boldsymbol{\tau}\cdot\mathbf{b}_\mu + \frac{e}{2}(1+\tau_3)A_\mu\right)\gamma^\mu\right]\psi \\ - \frac{\kappa}{3!}(g_{\rm s}\phi)^3 - \frac{\lambda}{4!}(g_{\rm s}\phi)^4 + \frac{\zeta}{4!}g_{\rm v}^4(V_\mu V^\mu)^2 \\ + \Lambda_{\rm v}\left(g_\rho^2\,\mathbf{b}_\mu\cdot\mathbf{b}^\mu\right)\left(g_{\rm v}^2 V_\nu V^\nu\right),\end{aligned} \tag{1}$$

where ψ represents the isodoublet nucleon field, A_μ is the photon field, and ϕ, V_μ, and $\mathbf{b}_\mu$ are the isoscalar-scalar σ-, isoscalar-vector ω-, and isovector-vector ρ-meson fields, respectively. The conventional Yukawa couplings between nucleons and mesons appear in the first line of Eq. (1). In the original Walecka model [62] it was sufficient to include the two isoscalar mesons to account for the saturation of symmetric nuclear matter at the mean field level. Later on, the model was extended by Horowitz and Serot [64,65] to include the isovector ρ meson and the photon. This formulation was successful in reproducing some ground-state properties with an accuracy that rivaled some of the most sophisticated nonrelativistic formulations of the time. However, in order to further improve the standing of the model, it was necessary to include nonlinear self and mixed interactions between the mesons; these nonlinear meson interactions are given in the second line of Eq. (1). For example, the introduction of the scalar self-interaction (κ and λ) by Boguta and Bodmer [66] reduces the incompressibility coefficient of symmetric nuclear matter from the unreasonably large value predicted by the Walecka model [36,62] to one that is consistent with measurements of the distribution of isoscalar monopole strength in medium to heavy nuclei. Moreover, Mueller and Serot [37] found it possible to build models with different values for the quartic ω-meson coupling (ζ) that reproduced the same nuclear properties at normal densities (such as the incompressibility coefficient) but that produced maximum neutron-star masses that differ by almost one solar mass. Hence, ζ can be used to efficiently tune the maximum neutron star mass [67,68]. Finally, the density dependence of the symmetry energy, which has important implications from nuclear structure to astrophysics, is governed by the ω-ρ mixed interaction ($\Lambda_{\rm v}$) [63,69]. RMF parameters for the two models employed in this work—FSUGold (or "FSU" for short) [61] and NL3 [39]—are given in Table I.

In the relativistic mean field limit, the meson fields satisfy (classical) nonlinear Klein-Gordon equations—with the relevant baryon densities acting as source terms. In turn, these meson fields provide the (scalar and vector) mean field potentials for the nucleons. Solution of the Dirac equation provide single-particle energies and wave functions, which are then used to construct the appropriate one-body densities that act as sources for the meson fields. This procedure is then repeated until self-consistency is achieved. In particular, the outcome from such a self-consistent procedure are a variety of ground-state properties, such as the spectrum of Dirac orbitals and density profiles. For a detailed description of the formalism and implementation of the RMF approach we refer the reader to Ref. [70]. We note, however, that the only inputs required for the implementation of the exact pairing approach are the single-particle energies of the valence orbitals.

B. Exact solution of the pairing problem

The RMF theory has been enormously successful in computing ground-state properties and collective excitations of even-even nuclei throughout the nuclear chart [39,40]. In addition, pairing correlations for the description of open shell nuclei are now routinely incorporated into the relativistic formalism via either a BCS or HFB approximation [see Ref. 19, and references contained therein]. However, it is the main purpose of this work to explore an alternative approach in which the pairing problem is solved exactly [34]. In particular—and in stark contrast to the BCS and HFB

TABLE I. Parameter sets for the two accurately calibrated relativistic mean field models used in the text: FSUGold [61] and NL3 [39]. The parameter κ and the meson masses $m_{\rm s}$, $m_{\rm v}$, and m_ρ are all given in MeV. The nucleon mass has been fixed at $M = 939$ MeV in both models.

Model	$m_{\rm s}$	$m_{\rm v}$	m_ρ	$g_{\rm s}^2$	$g_{\rm v}^2$	g_ρ^2	κ	λ	ζ	$\Lambda_{\rm v}$
FSU	491.500	782.500	763.000	112.1996	204.5469	138.4701	1.4203	+0.023762	0.06	0.030
NL3	508.194	782.501	763.000	104.3871	165.5854	79.6000	3.8599	−0.015905	0.00	0.000

approximations—particle number is exactly conserved in this formulation.

The general pairing Hamiltonian employed in this manuscript is given by the following expression:

$$H = \sum_{jm} \epsilon_j a^\dagger_{jm} a_{jm} - \frac{1}{4} \sum_{jj'} G_{jj'} \sum_{mm'} a^\dagger_{jm} \tilde{a}^\dagger_{jm} \tilde{a}_{j'm'} a_{j'm'}, \quad (2)$$

where ϵ_j is a set of RMF single-particle energies, and $G_{jj'}$ are pairing energies (for $j = j'$) and pair-transfer matrix elements (for $j \neq j'$). Note that in order to avoid double counting, the monopole contribution to the energy will need to be removed, as will be shown below. Nucleon creation and annihilation operators into a single-particle orbit labeled by quantum numbers j and m are described by $a^\dagger_{jm}$ and a_{jm}, respectively. Finally, $\tilde{a}_{jm}$ is a time-reversed operator defined as

$$\tilde{a}_{jm} = (-1)^{j-m} a_{j-m}. \quad (3)$$

The pairing problem with the above Hamiltonian can be solved exactly by introducing quasispin operators for each individual single-particle orbital [71,72]. In particular, the pairing Hamiltonian may be rewritten in terms of the quasispin operators as

$$H = \sum_j \epsilon_j \Omega_j + 2 \sum_j \epsilon_j L^z_j - \sum_{jj'} G_{jj'} L^+_j L^-_{j'}, \quad (4)$$

where $\Omega_j = (2j+1)/2$ represents the pair degeneracy of the j orbital and the three quasispin operators associated with such an orbital are defined as follows:

$$\begin{aligned} L^-_j &= \frac{1}{2} \sum_m \tilde{a}_{jm} a_{jm} \\ &= \frac{1}{2} \sqrt{2j+1} \sum_m \langle jm, j, -m | 00 \rangle a_{j-m} a_{jm}, \quad (5a) \\ L^+_j &= \frac{1}{2} \sum_m a^\dagger_{jm} \tilde{a}^\dagger_{jm} \\ &= \frac{1}{2} \sqrt{2j+1} \sum_m \langle jm, j, -m | 00 \rangle a^\dagger_{jm} a^\dagger_{j-m}, \quad (5b) \\ L^z_j &= \frac{1}{2} \sum_m \left(a^\dagger_{jm} a_{jm} - \frac{1}{2} \right) = \frac{1}{2} (N_j - \Omega_j). \quad (5c) \end{aligned}$$

From the above definition it is readily apparent that the operator L^+_j (L^-_j) creates (destroys) a nucleon pair of total angular momentum $J = 0$. Moreover, as the name indicates, the quasispin operators satisfy an SU(2) algebra with canonical commutation relations. That is,

$$[L^+_j, L^-_{j'}] = 2\delta_{jj'} L^z_j \quad \text{and} \quad \left[L^z_j, L^\pm_{j'} \right] = \pm \delta_{jj'} L^\pm_j. \quad (6)$$

An enormous advantage of introducing the concept of quasispin is that one can bring to bear the full power of the angular-momentum algebra into the problem [32,33]. Moreover, one can map the quasispin basis into the more intuitive "seniority" basis that is determined by the seniority quantum number s_j and the partial occupancy N_j of each orbital. Note that the seniority s_j of each level j represents the number of unpaired particles in such orbital. Given that the pairing Hamiltonian can only transfer pairs of particles, the seniority quantum number of each level is conserved. By the same token, the partial occupancy N_j of each orbital is not conserved. However, in contrast to the BCS and HFB formalism, the total number of particles is exactly conserved in this approach. This is one of the major advantages of the EP approach, as the exact conservation of the total number of particles avoids any reliance on complicated projection prescriptions. Finally, as the mapping between the seniority and quasispin bases is straightforward [30,72], one can evaluate matrix element of the Hamiltonian in the seniority basis by first transforming into the quasispin basis and then using the well known properties of the raising and lowering operators [34]. An overview of the exact-pairing approach and its applications may be found in Ref. [73]. In addition, a simple illustration of the EP method is given in the Appendix.

C. Relativistic mean field plus exact pairing formalism

Having briefly outlined the RMF theory and the EP method, we now use ^{116}Sn nucleus to illustrate the implementation of the combined RMF + EP approach. Since the tin isotopes have a closed proton shell, we regard the ^{100}Sn nucleus as an inert core and then limit the treatment to neutron-neutron (nn) pairing in the valence shell. In the particular case of ^{116}Sn, there are 16 valence neutrons residing in a shell consisting of 5 closely spaced orbitals ($1g_{7/2}$, $2d_{5/2}$, $2d_{3/2}$, $3s_{1/2}$, and $1h_{11/2}$) that can accommodate up to a maximum of 32 neutrons. For an RMF calculation without pairing correlations, these 16 neutrons fill up the $1g_{7/2}$, $2d_{5/2}$, and (half of the) $2d_{3/2}$ orbitals; the other two orbitals remain completely empty. Such a prescription seems rather unnatural given that the energy difference between filled and empty orbitals is comparable to the strength of the pairing interaction. In order to remedy this situation, we invoke pairing correlations to redistribute the valence particles among the 5 orbitals. To do so, we solve the pairing problem exactly using the energy spectrum (ϵ_j) generated by the RMF model as input to the pairing Hamiltonian. The Hilbert space for the EP problem is obtained by computing all possible ways to distribute the 8 neutron pairs among these 5 orbitals. This results in 110 different configurations which serve as the basis for the pairing Hamiltonian. We note that even though ^{116}Sn resides in the middle of the shell, the computational demands required to solve the EP problem exactly—namely, diagonalizing a 110×110 matrix—are very modest. Given that the pairing strengths in the G-matrix approach of Ref. [74] have been constrained by experiment, the only inputs required to compute all matrix elements of the pairing Hamiltonian are the single-particle energies predicted by the RMF model [34]. Diagonalizing the pairing Hamiltonian mixes all 110 configurations and results in a correlated lowest-energy state that is expressed as a linear combination of all these configurations. In particular, this leads to the *fractional occupancy* $\langle N_j \rangle$ of each orbital in the valence shell; this represents one of the hallmarks of pairing correlations. However, in contrast to other approaches to the pairing problem, in the EP formalism the total number of particles is exactly conserved: $N \equiv \sum_j \langle N_j \rangle$. Having obtained these new fractional occupancies, the RMF problem is solved

again, but now with updated baryon densities. These baryon densities generate new meson fields, new mean field potentials, and ultimately a new single-particle spectrum. The updated single-particle spectrum ϵ_j now serves as the new input to the EP problem which in turn generates a new set of partial occupancies. This iterative procedure is repeated until all fractional occupancies $\langle N_j \rangle$ and single-particle energies ϵ_j have converged. We note that the RMF + EP approach is self-consistent and particle number is conserved at every step in the iterative procedure.

Once the calculation has converged, one must then compute the pairing correlation energy. The correlation energy is obtained by subtracting from the ground-state energy of the pairing Hamiltonian E_0 the "naive" single-particle contribution. In this way the correlation energy accounts for the extra binding energy gained due to pairing. However, given that the diagonal pairing strengths G_{jj}—corresponding to the monopole part of EP problem—have already been included in the RMF calculation, one must also remove the monopole energy to avoid double counting. This yields the following form for the correlation energy [34]:

$$E_{\rm corr} = E_0 - \sum_j \epsilon_j \langle N_j \rangle + \sum_j \frac{G_{jj}}{2\Omega_j - 1} \frac{\langle N_j \rangle (\langle N_j \rangle - 1)}{2}. \tag{7}$$

Ultimately, the correlation energy is added to the corresponding RMF prediction and this is the nuclear binding energy that will be reported in Sec. III. Given that our calculations will focus on the tin isotopes, we adopt pairing strengths from the G-matrix calculation of Holt *et al.* [74]. Note that the values of relevance to neutron-neutron pairing have been listed in Table I of Ref. [73] and are also displayed for completeness in Table II. It has been shown that shell-model calculations with these pairing strengths yield an accurate spectroscopy for the tin isotopes in the $A = 120$–130 region; specifically, properties related to pairing correlations, such as the odd-even mass difference, the position of the first 2^+ state [2], as well as pairing vibrational 0^+ states [73] are all well reproduced. In general, the matrix elements of the pairing Hamiltonian are basis dependent and should be made consistent with the adopted mean field basis. Moreover, renormalization of the matrix elements is often required to account for the limitations of the chosen configuration space [2,44]. Nevertheless, for the results presented in this work such renormalization effects are small.

TABLE II. Pairing strengths $G_{jj'} = G_{j'j}$ (in MeV) for the model space of the tin isotopes ($A = 100$ to $A = 132$) [73] as determined from the G-matrix calculation of Holt *et al.* [74].

Orbital	$1g_{7/2}$	$2d_{5/2}$	$2d_{3/2}$	$3s_{1/2}$	$1h_{11/2}$
$1g_{7/2}$	0.2463	0.1649	0.1833	0.1460	0.2338
$2d_{5/2}$		0.2354	0.3697	0.1995	0.2250
$2d_{3/2}$			0.2032	0.2485	0.1761
$3s_{1/2}$				0.7244	0.1741
$1h_{11/2}$					0.1767

D. Constrained relativistic mean field theory

One of the central goals of the present paper is to investigate the effect of pairing correlations on the GMR energies of the tin isotopes. To do so we implement the newly developed *constrained*-RMF (CRMF) approach introduced in Ref. [60]. Although the constrained approach is unable to provide the full distribution of monopole strength, it is both accurate and efficient in estimating GMR energies. Indeed, the CRMF formalism that builds on the time-tested nonrelativistic formulation has been shown to provide an extremely favorable comparison against the predictions of a full relativistic RPA approach [60].

The *constrained* GMR energy is defined in terms of two moments of the distribution of strength:

$$E_{\rm con} = \sqrt{\frac{m_1}{m_{-1}}}, \tag{8}$$

where moments of the isoscalar distribution of monopole ($E0$) strength $R(\omega; E0)$ are given by

$$m_n(E0) \equiv \int_0^\infty \omega^n R(\omega; E0)\, d\omega. \tag{9}$$

Note that we distinguish here the constrained energy from the corresponding *centroid* energy that is customarily defined as $E_{\rm cen} = m_1/m_0$. In particular, assuming a simple Lorentzian distribution of strength one obtains

$$E_{\rm cen}({\rm RPA}) = \omega_0 \quad \text{and} \quad E_{\rm con}({\rm RPA}) = \sqrt{\omega_0^2 + \Gamma^2/4}, \tag{10}$$

where ω_0 is the resonance energy and Γ the full width at half maximum.

The great virtue of the constrained approach is that both of the moments involved in $E_{\rm con}$ may be directly computed from ground-state observables. In particular, using Thouless's theorem one may compute the m_1 moment (also known as the energy weighted sum) by evaluating a suitably defined double commutator [45]. This procedure yields

$$\begin{aligned} m_1(E0) &\equiv \int_0^\infty \omega R(\omega; E0)\, d\omega = \frac{2\hbar^2}{M} A \langle r^2 \rangle \\ &= \frac{2\hbar^2}{M} \int r^2 \rho(\mathbf{r})\, d^3r, \end{aligned} \tag{11}$$

where M is the nucleon mass and $\rho(\mathbf{r})$ the ground-state baryon density. Similarly, by invoking the "dielectric theorem" the m_{-1} moment may be written as follows [15]:

$$\begin{aligned} m_{-1}(E0) &\equiv \int_0^\infty \omega^{-1} R(\omega; E0)\, d\omega \\ &= -\frac{1}{2} \left[\frac{d}{d\eta} \int r^2 \rho(\mathbf{r}; \eta)\, d^3r \right]_{\eta=0}. \end{aligned} \tag{12}$$

Here $\rho(\mathbf{r}; \eta)$ is a slightly perturbed ground-state density obtained from solving the RMF equations by adding a constrained one-body term $V_{\rm con}(r) = \eta r^2$ to the repulsive vector interaction [60]. Such a constrained term "squeezes" the nucleus, making it more compact, thereby mimicking the characteristic radial density oscillation of the GMR. Clearly, the constrained approach is significantly faster than

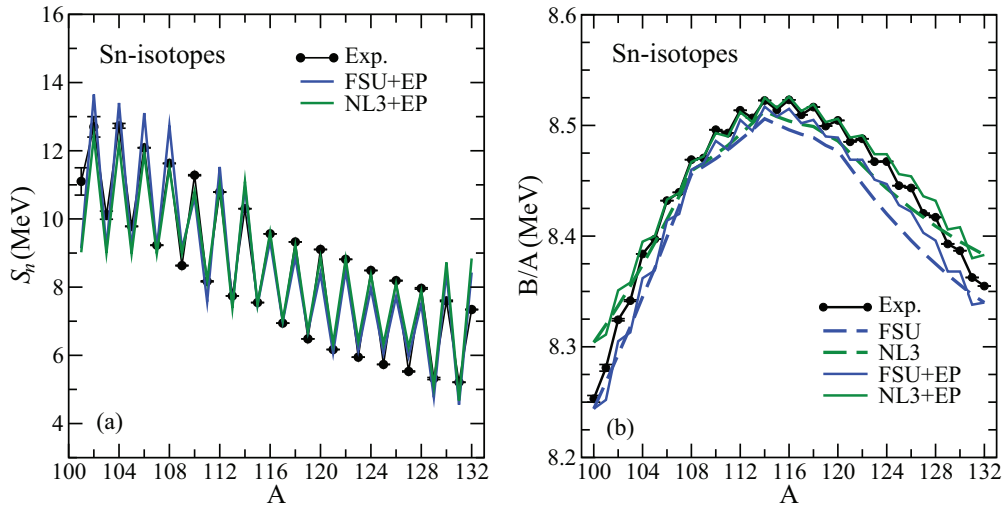

FIG. 1. (Color online) Odd-even staggering of the one-neutron separation energy (left panel) and binding energy per nucleon (right panel) along the isotopic chain in tin as predicted by the FSUGold [61] and NL3 [39] models—supplemented with an exact treatment of pairing correlations. Experimental results are from Ref. [76].

the RPA (or quasiparticle RPA) as the required moments of the distribution are calculated directly from suitably modified ground-state properties, rather than from the full distribution of monopole strength. To study the impact of pairing correlations on the GMR energies of the tin isotopes, ground-state densities will be computed in the combined RMF + EP formalism, as we describe in the above section.

III. RESULTS

To demonstrate the applicability and utility of the combined RMF + EP approach we now display calculations for the isotopic chain in tin, from $A = 100$ to $A = 132$. As mentioned earlier, we regard the doubly magic ^{100}Sn nucleus as an inert core and then concentrate on the impact of *nn* pairing on the $N \leqslant 32$ neutrons in the valence shell. The RMF models listed in Table I are fairly successful in reproducing ground-state properties (such as binding energies and charge radii) of a variety of nuclei throughout the nuclear chart. However, their predictions for some bulk properties of nuclear matter and neutron-star observables differ considerably. For example, the incompressibility coefficient of symmetric nuclear matter is predicted by FSUGold to be $K_0 = 230$ MeV whereas NL3 suggests $K_0 = 271$ MeV. Moreover, the slope of the symmetry energy L—which controls the softening of the GMR energy along an isotopic chain [53,54,75]—is also significantly different: $L = 61$ MeV for FSUGold and $L = 118$ MeV for NL3. Thus, these two models—one soft and one stiff—provide an adequate representative set for the illustration of the method.

On the left-hand panel of Fig. 1 we show one of the classical signatures of pairing correlations: the odd-even staggering of the neutron separation energy along the isotopic chain in tin; experimental data are from the compilation given in Ref. [76]. Note that for odd-A nuclei the unpaired neutron is placed in the single-particle orbital that reproduces the experimental angular momentum and parity of the ground state [76]. In the case of even-A nuclei all neutrons are paired. This odd-even difference gives rise to the characteristic staggering observed in the one-neutron separation energy. That is, in the case of an even-A nucleus, one must provide the energy necessary to break a pair before the neutron can be excited into the continuum. In contrast, for odd-A nuclei there is no additional cost associated with breaking a pair. Figure 1 suggests that the energy required to break a pair is about 3 MeV, which is the typical strength associated with the residual interaction. Moreover, it can be seen that for the stable $A = 112$–124 nuclei the results are in good agreement with experiment. However, deviations of about 1MeV seem to emerge at the two ends of the isotopic chain. We would like to point out that the ground-state spin of some of those unstable odd-A nuclei is uncertain. In addition, if the neutron $1g_{9/2}$ orbital (which so far has been assumed inert) is incorporated into the pairing calculation, the discrepancies in the light isotopes are expected to disappear. Similarly, we expect that the predictions for the heavier isotopes will improve as one includes higher neutron orbitals. On the right-hand panel of Fig. 1 we display the binding energy per nucleon along the isotopic chain. Many of the same features already evident in the one-neutron separation energy are also manifest in this observable. However, in this case we also display the predictions from the RMF models *without* pairing correlations. As expected—and in sharp contrast to the experimental data—the predicted A dependence is smooth and devoid of the "zigzag" structure. Naturally, pairing correlations tend to increase the binding energy relative to the pure RMF predictions. However, in some special situations—such as that of an unpaired particle or hole—this may not be the case due to the placement of the unpaired nucleon; see for example the cases of ^{101}Sn, ^{103}Sn, and ^{131}Sn in Fig. 1(b). Indeed, for the RMF + EP predictions, the placement of the unpaired nucleon is set by the experimentally known spin and parity of the ground state. In contrast, in the RMF approach all single-particle levels are filled sequentially in accordance to the Pauli exclusion principle; this fact may occasionally give rise to unconventional behavior.

TABLE III. Single-particle occupancies $\langle N_j \rangle$ of the orbitals in the valence shell for the stable even-even Sn isotopes. Results are presented for FSUGold [61] and (separated by a "/") for NL3 [39].

	^{112}Sn	^{114}Sn	^{116}Sn	^{118}Sn	^{120}Sn	^{122}Sn	^{124}Sn
$1g_{7/2}$	7.80/7.58	7.89/7.80	7.88/7.80	7.89/7.81	7.92/7.84	7.91/7.85	7.92/7.87
$2d_{5/2}$	3.64/3.72	5.46/5.42	5.54/5.49	5.66/5.58	5.79/5.68	5.79/5.72	5.81/5.77
$2d_{3/2}$	0.28/0.32	0.33/0.36	1.24/1.30	2.31/2.24	3.42/3.01	3.52/3.30	3.62/3.50
$3s_{1/2}$	0.08/0.09	0.11/0.12	0.86/0.72	1.38/1.15	1.77/1.52	1.81/1.66	1.84/1.76
$1h_{11/2}$	0.20/0.29	0.21/0.30	0.47/0.70	0.76/1.21	1.11/1.96	2.97/3.46	4.80/5.11

Another critical signature of pairing correlations is the fractional occupancy of the single-particle orbits. Thus, the predicted fractional occupancies $\langle N_j \rangle$ for the five neutron orbitals forming the valence space are displayed in Table III for all stable, even-A tin isotopes. Predictions are presented for FSUGold and (separated by a "/") for NL3. As shown in the table, pairing correlations can modify the occupancies by as much as one neutron relative to the naive mean field expectations. In particular, such changes may have a significant impact on the novel "bubble" structure and concomitant quenching of the spin-orbit splitting of low-j orbitals [77–80]. Indeed, in Fig. 2 we exhibit the ground-state neutron density of ^{118}Sn as predicted by both RMF models with and without the inclusion of pairing correlations. In the extreme mean field limit, ^{118}Sn consists of filled $1g_{7/2}$, $2d_{5/2}$, and $2d_{3/2}$ orbitals. In particular, the absence of $3s_{1/2}$ neutrons yields the bubble structure (manifested as a central depression) in the neutron density. In turn, such a central depression leads to a modification of the spin-orbit potential that results in a quenching of the spin-orbit splitting between the $2p_{3/2}$ and $2p_{1/2}$ proton orbitals: 0.85 MeV for FSUGold and 0.77 MeV for NL3. However, the $3s_{1/2}$ orbital lies within $\sim$0.5 MeV of the $2d_{3/2}$ orbital, so the mixing induced by the pairing interaction is very efficient (see Table III). Indeed, with more than one neutron transferred to the $3s_{1/2}$ orbital, the bubble structure of ^{118}Sn disappears entirely. Moreover, the $2p_{3/2}$-$2p_{1/2}$ spin-orbit splitting increases by more than 50% to 1.33 MeV for both FSUGold and NL3. Note, however, that the occupancy of the $3s_{1/2}$ orbital in both ^{112}Sn and ^{114}Sn remains small so their bubble structure is preserved—although not as pronounced as in the case of ^{118}Sn.

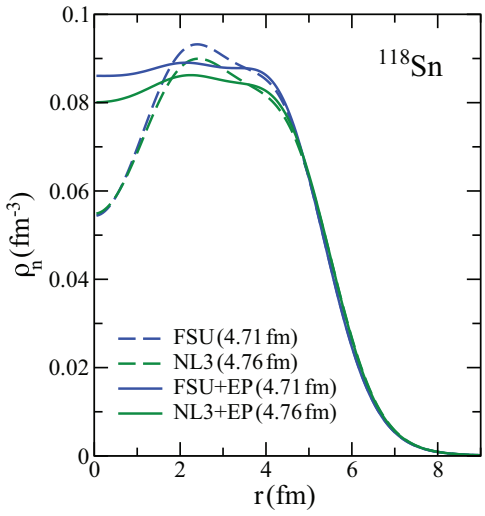

FIG. 2. (Color online) Neutron density of ^{118}Sn as predicted by the FSUGold [61] and NL3 [39] models. Predictions are displayed with (solid lines) and without (dashed lines) pairing correlations. Quantities enclosed in parenthesis represent the model predictions for the neutron root-mean-square radius.

We finish this section by addressing the role of pairing correlations in explaining the softness of the tin isotopes [50,51]. The study of pairing correlation on the GMR energies of the tin isotopes dates back to the work of Civitarese *et al.* [81] in the early 1990s. By employing a quasiparticle-RPA formalism, the authors reported a small shift of about 100 to 150 keV in the monopole energies due to pairing correlations. Recently, the role of pairing correlations has been revisited as a possible mechanism to soften the GMR energies of these superfluid nuclei [55–59]. Thus, it seems natural to examine this critical issue within the context of the RMF + EP approach introduced here.

To investigate the effect of pairing correlations on the monopole energies we invoke the newly developed constrained-RMF approach introduced in Ref. [60]. As already alluded in Sec. II D, the convenience of the constrained approach stems from the accurate and efficient estimation of GMR energies without the need to generate the full distribution of monopole strength. Indeed, as indicated in Eqs. (11) and (12), GMR energies may be computed directly from the mean-square radius of the *ground-state* distribution. Recently, excellent results were obtained as the CRMF approach was compared against the predictions from a relativistic RPA calculation [60]. To examine the impact of pairing correlations on the GMR energies, the ground-state densities that serve as the input for the constrained approach will now be calculated using the RMF + EP formalism. A first glance at Fig. 2 may suggest that pairing correlations could have a dramatic effect on the GMR energies. However, upon closer inspection one realizes that it is the mean-square radius of the ground-state density that is of relevance to the GMR energies. Hence, the r^4 weighting of the density, namely,

$$\langle r^2 \rangle = \frac{4\pi}{A} \int r^4 \rho(r)\, dr, \tag{13}$$

washes out the dramatic effect observed in the central density. Indeed, we find no modification to the mean-square radius from pairing correlations; the root-mean-square radius of the neutron density of ^{118}Sn is displayed in Fig. 2. We note that

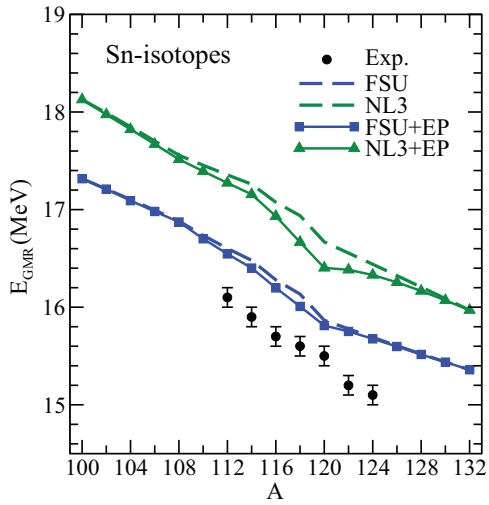

FIG. 3. (Color online) Giant monopole energies in the even-even Sn isotopes with and without pairing correlations compared against the experimental results of Li *et al.* [50]. Predictions from both FSUGold [61] and NL3 [39]—with and without pairing correlations—overestimate the experimental data.

this behavior is not exclusive to ^{118}Sn as no significant change in the neutron radius of the tin isotopes was found in this work.

GMR energies for the whole isotopic chain in tin—from $A = 100$ to $A = 132$—are displayed in Fig. 3 alongside the experimental results for the stable even-A isotopes [50]. As the number of neutrons increases, the GMR energy decreases monotonically. In this regard two points are worth emphasizing: (a) the value of the centroid energy in ^{112}Sn and (b) the softening of the mode as a function of A. First, given that the neutron excess in ^{112}Sn is small, the value of its centroid energy is mostly sensitive to the incompressibility coefficient of symmetric nuclear matter. This is clearly reflected in the model predictions; recall that $K_0 = 230$ MeV for FSUGold and $K_0 = 271$ MeV for NL3. However, even the significantly softer FSUGold model overestimates the centroid energy in ^{112}Sn by about 0.3 MeV. Second, the experiment suggests a very rapid softening that is not reproduced by either of the models. Note that the falloff with A is largely controlled by the slope of the symmetry energy L [54]. Thus, whereas the falloff predicted by NL3 may indeed be slightly faster than that of FSUGold, it is clearly nowhere as fast as required by the experiment. Thus, although we have gone beyond a mean field plus RPA description, Fig. 3 indicates that the impact of pairing correlations on the GMR energies is fairly small—especially in the case of FSUGold. Indeed, the largest correction due to pairing is about 275 keV for NL3 and about 125 keV for FSUGold. Given that in the constrained approach the GMR energy is driven by the mean-square radius of the density distribution, it hardly comes as a surprise that pairing correlations play a minor role. Moreover, although both RMF models have been accurately calibrated, NL3 predicts a valence spectrum that is in general more compressed than the one predicted by FSUGold. Thus, pairing correlations are more quenched in FSUGold than in NL3. In addition, from ^{102}Sn to ^{114}Sn the valence neutrons reside in the $1g_{7/2}$ and $2d_{5/2}$ orbitals—which are relatively well separated from the $2d_{3/2}$, $3s_{1/2}$, and $1h_{11/2}$ orbitals. Thus, pairing correlations play a minor role in populating the three higher orbitals (see Table III). However, once the higher orbitals start to be populated, pairing correlations become very efficient at redistributing nn -pairs, especially among the quasidegenerate $2d_{3/2}$ and $3s_{1/2}$ orbitals. This is particularly true in the middle of the shell, namely, from ^{116}Sn to ^{120}Sn. After that the effect from pairing correlations weakens because transitions to the partially occupied $1h_{11/2}$ orbital become Pauli blocked. Note that contrary to the predictions of Ref. [56]—where constrained HFB calculations using Skyrme functionals and a zero-range surface pairing force were performed—we do not observe a rapid stiffening of the mode (in the form of a prominent peak) as one reaches the doubly-magic nucleus ^{132}Sn.

IV. CONCLUSIONS

In this work we introduced a novel hybrid approach to compute the properties of open shell nuclei. The method consists of a relativistic mean field approximation supplemented with an exact treatment of pairing correlations. One of the major advantages of the exact treatment is that it conserves the number of particles. This avoids any reliance on complicated prescriptions that must be used to project out the correct number of particles. Moreover, the EP approach works well even for nuclei with typical single-particle-energy spacings greater than the pairing strengths—a limit in which both BCS and HFB tend to fail. Finally, the combined RMF + EP approach is simple to implement. One starts by computing the single-particle spectrum using a traditional mean field approach. Once the valence shell is identified, then one passes the relevant single-particle energies to the exact pairing routine—which redistributes pairs among the valence orbitals. The newly obtained fractional occupancies then generate a new set of baryon densities that ultimately yield an updated single-particle spectrum. This updated spectrum now serves as input to the exact pairing routine and the procedure is repeated until self-consistency is achieved.

The utility and applicability of the RMF + EP approach was demonstrated using the long chain of tin isotopes as an example. Predictions for both ground-state properties and GMR energies were compared against experimental results. In the case of ground-state properties, results were presented for the characteristic odd-even staggering of the one-neutron separation energy and binding energies across the full isotopic chain: from ^{100}Sn to ^{132}Sn. We find that our predictions compare very favorably against the experimental results. In addition, we presented results for the single-particle occupancies of the relevant neutron orbitals and investigated their impact on the alleged nuclear bubble structure. In particular, we concluded that the bubble structure observed in the "mean field" neutron density of ^{118}Sn is completely eliminated with the inclusion of pairing correlations. However, we find that the bubble structure of both ^{112}Sn and ^{114}Sn, although not as pronounced as in the case of ^{118}Sn, is still maintained.

We also investigated the role of pairing correlations on the possible softening of the GMR energies in the tin isotopes. To do so, we adopted the recently developed constrained-RMF

framework that has been shown to accurately reproduce GMR energies obtained with the more sophisticated RPA approach. The great merit of the constrained approach is that GMR energies can be accurately and efficiently computed from the mean-square radius of the *ground-state* density distribution. Thus, in this work we investigated the role of pairing correlations by supplying the CRMF approach with densities computed in the RMF + EP framework. As has been extensively documented, models that reproduce the GMR energies in both ^{90}Zr and ^{208}Pb overestimate the corresponding monopole energies along the isotopic chain in tin. Given that pairing correlations have been proposed as a possible solution to the softening of these superfluid nuclei, GMR energies along the isotopic chain in tin—from ^{100}Sn to ^{132}Sn—were computed using the combined RMF + EP formalism. We concluded, as many have done before us, that pairing correlations provide (if at all) a very mild softening of the mode. Within the constrained approach the explanation for this behavior is rather simple. Whereas pairing correlations modify the ground-state density distribution, most of these modifications are limited to the nuclear interior. Given that the constrained energy is driven by the mean-square radius of the density distribution—which is largely insensitive to the nuclear interior—pairing correlations play a minor role in the softening of the mode. Thus, we conclude that pairing correlations cannot be the explanation behind the question, "Why is tin so soft?"

In summary, we have introduced a novel RMF + EP approach to compute ground-state properties and collective excitations of open shell nuclei. The approach is elegant and straightforward, and its implementation fast and reliable. Moreover, particle-number conservation is strictly maintained, so the approach is not hindered by complicated projection prescriptions required in other formulations. We are confident that the combined RMF + EP approach introduced here provides a simple and powerful framework for the exploration of the limits of nuclear existence, such as in the study of superheavy nuclei and of nuclei near the drip lines.

ACKNOWLEDGMENTS

This work was supported in part by the United States Department of Energy under Grants No. DE-FG05-92ER40750 and No. DE-SC0009883.

APPENDIX: TOY MODEL OF THE EXACT PAIRING ALGORITHM

To illustrate how the exact pairing algorithm is implemented we present here a toy model consisting of four neutrons residing in two single-particle orbitals, such as $2d_{3/2}$ (label 1) and $3s_{1/2}$ (label 2). This example may reflect the simplified situation in which ^{114}Sn may be assumed as an inert core and one is interested in studying the structure of ^{118}Sn—particularly the occupancy of the quasi-degenerate $2d_{3/2}$ and $3s_{1/2}$ orbitals. Assuming that all four neutrons are paired, i.e., both orbitals have seniority zero, there are only two allowed configurations:

$$|a\rangle = |N_1 = 4, N_2 = 0\rangle \quad \text{and} \quad |b\rangle = |N_1 = 2, N_2 = 2\rangle. \tag{A1}$$

Matrix elements of the pairing Hamiltonian in the seniority basis are now obtained from the general expressions derived in Ref. [34]. For example, the diagonal matrix elements of the pairing Hamiltonian are given by

$$\langle N_1, N_2|H|N_1, N_2\rangle = \sum_{j=1}^{2}\left[\epsilon_j N_j - \frac{G_{jj}}{4} N_j(2\Omega_j - N_j + 2)\right], \tag{A2}$$

where ϵ_j are single-particle energies, G_{jj} are (diagonal) pairing strengths, and Ω_j is the pair degeneracy of orbital j; $\Omega_1 = 2$ and $\Omega_2 = 1$. Similarly, the off-diagonal matrix elements are given by

$$\langle N_1 + 2, N_2 - 2|H|N_1, N_2\rangle = -\frac{G_{12}}{4}\sqrt{N_2(2\Omega_2 - N_2 + 2)(2\Omega_1 - N_1)(N_1+2)}, \tag{A3}$$

where now G_{12} is the pair-transfer strength. By assuming a constant pairing strength $G_{jj'} \equiv g$ (with $g > 0$) the 2×2 pairing Hamiltonian takes the following simple form:

$$H = \begin{pmatrix} 4\epsilon_1 - 2g & -\sqrt{2}g \\ -\sqrt{2}g & 2\epsilon_1 + 2\epsilon_2 - 3g \end{pmatrix} = E\mathbb{1} + \begin{pmatrix} -\epsilon & -\sqrt{2}g \\ -\sqrt{2}g & \epsilon \end{pmatrix}, \tag{A4}$$

where we have introduced the following definitions (with $\Delta \equiv \epsilon_2 - \epsilon_1$):

$$E \equiv 4\epsilon_1 + \Delta - \tfrac{5}{2}g \quad \text{and} \quad \epsilon \equiv \Delta - \tfrac{1}{2}g. \tag{A5}$$

Diagonalizing the pairing Hamiltonian yields the following value for the ground-state energy and for its corresponding eigenstate:

$$E_0 = E - \xi \equiv E - \sqrt{\epsilon^2 + 2g^2}, \tag{A6a}$$

$$|E_0\rangle = \sqrt{\frac{\xi + \epsilon}{2\xi}}\,|N_1 = 4, N_2 = 0\rangle + \sqrt{\frac{\xi - \epsilon}{2\xi}}\,|N_1 = 2, N_2 = 2\rangle. \tag{A6b}$$

In a mean field calculation without pairing correlations, the four neutrons would occupy the lowest $2d_{3/2}$ orbital with the lowest energy being equal to $E_0 = 4\epsilon_1$. Pairing correlations reduce the ground-state energy at the expense of redistributing

TABLE IV. Ground-state energy of the pairing Hamiltonian and corresponding single-particle occupancies for different values of Δ/g.

Δ/g	$(E_0 - 4\epsilon_1)/g$	$\langle N_1\rangle$	$\langle N_2\rangle$
1/2	−3.414	3.000	1.000
1	−3.000	3.333	0.667
2	−2.562	3.728	0.272
4	−2.275	3.927	0.073
8	−2.132	3.983	0.017
16	−2.064	3.996	0.004

the four neutrons among the two valence orbitals. In this way the average occupancy of the two orbitals becomes

$$\langle N_1 \rangle = 3 + \frac{\epsilon}{\xi} \quad \text{and} \quad \langle N_2 \rangle = 1 - \frac{\epsilon}{\xi}. \tag{A7}$$

Note that the fractional occupancies of the single-particle orbits depend exclusively on the ratio of Δ/g. In Table IV we list (properly scaled) ground-state energies as well as fractional occupancies for the two valence orbitals. At values of $\Delta/g \simeq 1$ the ground state is well correlated and the occupancy of the lowest orbital gets significantly depleted. In contrast, for $\Delta/g \gg 1$, the single-particle gap is significantly larger than the pairing strength and the occupancy of the lowest state returns to its mean field value of 4.

[1] Maria Goeppert Mayer, Phys. Rev. **78**, 16 (1950).
[2] D. J. Dean and M. Hjorth-Jensen, Rev. Mod. Phys. **75**, 607 (2003).
[3] A. Bohr and B. R. Mottelson, *Nuclear Structure* (World Scientific, New Jersey, 1998).
[4] J. Dobaczewski, W. Nazarewicz, T. R. Werner, J. F. Berger, C. R. Chinn, and J. Decharge, Phys. Rev. C **53**, 2809 (1996).
[5] M. Pfutzner, M. Karny, L. V. Grigorenko, and K. Riisager, Rev. Mod. Phys. **84**, 567 (2012).
[6] S. Hofmann and G. Munzenberg, Rev. Mod. Phys. **72**, 733 (2000).
[7] Y. T. Oganessian *et al.*, Phys. Rev. Lett. **104**, 142502 (2010).
[8] J. Bardeen, L. Cooper, and J. Schrieffer, Phys. Rev. **108**, 1175 (1957).
[9] A. Bohr, B. Mottelson, and D. Pines, Phys. Rev. **110**, 936 (1958).
[10] S. Belyaev, K. Dan. Vidensk. Selsk. Mat-fys. Medd. **31**, 641 (1959).
[11] A. Migdal, Nucl. Phys. **13**, 655 (1959).
[12] F. Tondeur, Nucl. Phys. A **315**, 353 (1979).
[13] R. C. Nayak and J. M. Pearson, Phys. Rev. C **52**, 2254 (1995).
[14] N. N. Bogoliubov, Dokl. Akad. Nauk SSSR **119**, 244 (1959).
[15] P. Ring and P. Schuck, *The Nuclear Many-Body Problem* (Springer, New York, 2004).
[16] T. Duguet, P. Bonche, P.-H. Heenen, and J. Meyer, Phys. Rev. C **65**, 014310 (2001).
[17] T. Duguet, P. Bonche, P.-H. Heenen, and J. Meyer, Phys. Rev. C **65**, 014311 (2001).
[18] N. Paar, P. Ring, T. Niksic, and D. Vretenar, Phys. Rev. C **67**, 034312 (2003).
[19] D. Vretenar, A. Afanasjev, G. Lalazissis, and P. Ring, Phys. Rep. **409**, 101 (2005).
[20] J. Meng, H. Toki, S. G. Zhou, S. Q. Zhang, W. H. Long, and L. S. Geng, Prog. Part. Nucl. Phys. **57**, 470 (2006).
[21] L. Li, J. Meng, P. Ring, E.-G. Zhao, and S.-G. Zhou, Phys. Rev. C **85**, 024312 (2012).
[22] H. J. Lipkin, Ann. Phys. (N.Y.) **31**, 525 (1960).
[23] Y. Nogami, Phys. Rev. **134**, 313 (1964).
[24] M. Anguiano, J. L. Egido, and L. M. Robledo, Nucl. Phys. A **696**, 467 (2001).
[25] R. W. Richardson, Phys. Lett. **3**, 277 (1963).
[26] R. W. Richardson, Phys. Lett. **5**, 82 (1963).
[27] R. W. Richardson, Phys. Lett. **14**, 325 (1965).
[28] J. Dukelsky, S. Pittel, and G. Sierra, Rev. Mod. Phys. **76**, 643 (2004).
[29] F. Pan, J. Draayer, and W. Ormand, Phys. Lett. B **422**, 1998 (1998).
[30] G. Racah, Phys. Rev. **62**, 438 (1942).
[31] G. Racah, Phys. Rev. **63**, 367 (1943).
[32] A. K. Kerman, R. D. Lawson, and M. H. Macfarlane, Phys. Rev. **124**, 162 (1961).
[33] H. Chen, T. Song, and D. J. Rowe, Nucl. Phys. A **582**, 181 (1995).
[34] A. Volya, B. A. Brown, and V. Zelevinsky, Phys. Lett. B **509**, 37 (2001).
[35] A. Volya, B. A. Brown, and V. Zelevinsky, Prog. Theor. Phys. Suppl. **146**, 636 (2002).
[36] B. D. Serot and J. D. Walecka, Adv. Nucl. Phys. **16**, 1 (1986).
[37] H. Mueller and B. D. Serot, Nucl. Phys. A **606**, 508 (1996).
[38] B. D. Serot and J. D. Walecka, Int. J. Mod. Phys. E **6**, 515 (1997).
[39] G. A. Lalazissis, J. Konig, and P. Ring, Phys. Rev. C **55**, 540 (1997).
[40] G. A. Lalazissis, S. Raman, and P. Ring, At. Data Nucl. Data Tables **71**, 1 (1999).
[41] H. Molique and J. Dudek, Phys. Rev. C **56**, 1795 (1997).
[42] J. Meng, J. Y. Guo, L. Liu, and S. Q. Zhang, Front. Phys. China **1**, 38 (2006).
[43] J. Y. Zeng and T. S. Cheng, Nucl. Phys. A **405**, 1 (1983).
[44] Z.-H. Zhang, X.-T. He, J.-Y. Zeng, E.-G. Zhao, and S.-G. Zhou, Phys. Rev. C **85**, 014324 (2012).
[45] M. N. Harakeh and A. van der Woude, *Giant Resonances: Fundamental High-Frequency Modes of Nuclear Excitation* (Clarendon, Oxford, 2001).
[46] D. H. Youngblood, H. L. Clark, and Y.-W. Lui, Phys. Rev. Lett. **82**, 691 (1999).
[47] Y. W. Lui, D. H. Youngblood, Y. Tokimoto, H. L. Clark, and B. John, Phys. Rev. C **70**, 014307 (2004).
[48] M. Uchida *et al.*, Phys. Lett. B **557**, 12 (2003).
[49] M. Uchida, H. Sakaguchi, M. Itoh, M. Yosoi, T. Kawabata *et al.*, Phys. Rev. C **69**, 051301 (2004).
[50] T. Li *et al.*, Phys. Rev. Lett. **99**, 162503 (2007).
[51] T. Li *et al.*, Phys. Rev. C **81**, 034309 (2010).
[52] D. Patel, U. Garg, M. Fujiwara, H. Akimune, G. Berg *et al.*, Phys. Lett. B **718**, 447 (2012).
[53] J. Piekarewicz, J. Phys. G **37**, 064038 (2010).
[54] J. Piekarewicz, arXiv:1307.7746.
[55] J. Li, G. Colo, and J. Meng, Phys. Rev. C **78**, 064304 (2008).
[56] E. Khan, Phys. Rev. C **80**, 011307 (2009).
[57] E. Khan, Phys. Rev. C **80**, 057302 (2009).
[58] E. Khan, J. Margueron, G. Colò, K. Hagino, and H. Sagawa, Phys. Rev. C **82**, 024322 (2010).
[59] P. Vesely, J. Toivanen, B. G. Carlsson, J. Dobaczewski, N. Michel, and A. Pastore, Phys. Rev. C **86**, 024303 (2012).
[60] W.-C. Chen, J. Piekarewicz, and M. Centelles, Phys. Rev. C **88**, 024319 (2013).
[61] B. G. Todd-Rutel and J. Piekarewicz, Phys. Rev. Lett. **95**, 122501 (2005).
[62] J. D. Walecka, Ann. Phys. (N.Y.) **83**, 491 (1974).
[63] C. J. Horowitz and J. Piekarewicz, Phys. Rev. Lett. **86**, 5647 (2001).
[64] B. D. Serot, Phys. Lett. B **86**, 146 (1979).

[65] C. J. Horowitz and B. D. Serot, Nucl. Phys. A **368**, 503 (1981).
[66] J. Boguta and A. R. Bodmer, Nucl. Phys. A **292**, 413 (1977).
[67] P. Demorest, T. Pennucci, S. Ransom, M. Roberts, and J. Hessels, Nature (London) **467**, 1081 (2010).
[68] J. Antoniadis, P. C. Freire, N. Wex, T. M. Tauris, R. S. Lynch *et al*., Science **340**, 6131 (2013).
[69] C. J. Horowitz and J. Piekarewicz, Phys. Rev. C **64**, 062802 (2001).
[70] B. G. Todd and J. Piekarewicz, Phys. Rev. C **67**, 044317 (2003).
[71] P. W. Anderson, Phys. Rev. **112**, 1900 (1958).
[72] A. K. Kerman, Ann. Phys. (N.Y.) **12**, 300 (1961).
[73] V. Zelevinsky and A. Volya, Phys. At. Nucl. **66**, 1781 (2003).
[74] A. Holt, T. Engeland, M. Hjorth-Jensen, and E. Osnes, Nucl. Phys. A **634**, 41 (1998).
[75] J. Piekarewicz and M. Centelles, Phys. Rev. C **79**, 054311 (2009).
[76] National Nuclear Data Center, Brookhaven National Laboratory.
[77] B. G. Todd-Rutel, J. Piekarewicz, and P. D. Cottle, Phys. Rev. C **69**, 021301 (2004).
[78] L. Gaudefroy *et al*., Phys. Rev. Lett. **97**, 092501 (2006).
[79] J. Piekarewicz, J. Phys. G **33**, 467 (2007).
[80] M. Grasso *et al*., Phys. Rev. C **79**, 034318 (2009).
[81] O. Civitarese, A. G. Dumrauf, M. Reboiro, P. Ring, and M. M. Sharma, Phys. Rev. C **43**, 2622 (1991).